Proceedings of ICFDP7:
7th International Conference on Fluid Dynamics and Propulsion
December 18-20, 2001, Cairo, EGYPT

ICFDP7-2001053

A NUMERICAL STUDY ON THE SIMILARITY OF LAMINAR FLOWS IN ORTHOGONALLY ROTATING RECTANGULAR DUCTS AND STATIONARY CURVED RECTANGULAR DUCTS OF ARBITRARY ASPECT RATIO

GONG HEE LEE
Department of Mechanical Engineering, POSTECH,
San31, Hyoja Dong, Pohang, 790-784, KOREA
Email: ghlee2@postech.ac.kr

JE HYUN BAEK
Department of Mechanical Engineering, POSTECH,
San31, Hyoja Dong, Pohang, 790-784, KOREA
Email: jhbaek@postech.ac.kr

ABSTRACT

The present study showed that a quantitative analogy of the fully developed laminar flows in orthogonally rotating rectangular ducts and stationary curved rectangular ducts of arbitrary aspect ratio could be established. In order to clarify the similarity of the two flows, the dimensionless parameters $K_{LR}=Re/(Ro)^{1/2}$ and Rossby number, $Ro=w_m/Wd$, in a rotating straight duct were used as a set corresponding to Dean number $K_{LC}=Re/l^{1/2}$ and curvature ratio $l = R/d$ in a stationary curved duct. Under the condition that the value of Rossby number and curvature ratio was large enough, the flow field satisfied the 'asymptotic invariance property'; there were strong quantitative similarities between the two flows such as friction factors, flow patterns, and maximum axial velocity magnitudes for the same values of K_{LR} and K_{LC}.

NOMENCLATURE

A	aspect ratio $= b/a$
a	width of duct cross-section
b	height of duct cross-section
d	hydraulic diameter of the rectangular duct $=2ab/(a+b)$
f	Fanning friction factor
f_0	friction factor for a stationary straight duct
K_{LR}	dimensionless parameter for laminar flow in a rotating duct $=Re/(Ro)^{1/2}$
K_{LC}	dimensionless parameter for laminar flow in a curved duct or Dean number $=Re/l^{1/2}$
p	static pressure
p^*	modified pressure $=p-(x^2+z^2)/2$
R	mean radius of curvature
Re	Reynolds number $=w_m d/n$
Ro	Rossby number $=w_m/Wd$
u,v,w	velocity components in the direction of x,y,z
V_s	secondary flow velocity $=(u^2+v^2)^{1/2}$
w_m	mean velocity

Greek Symbols

l	curvature ratio $=R/d$
n	kinematic viscosity of the fluid
r	density of the fluid
W	angular velocity

Superscript

-	average value

INTRODUCTION

Fluid flows in both rotating and curved ones have attracted much attention because of their relevance to various engineering applications. These include flows through the cooling passages of turbine blades, blade passages of turbomachinery, heat exchangers and refrigeration equipments. These flows of practical interest are characterized by the occurrence of a secondary flow due to the system rotation and/or curvature effects. Such a secondary flow not only causes a reduction in the volumetric flow rate for a fixed pressure difference, but also redistributes the axial velocity field. In the case of the fully developed flow through a straight duct rotating about an axis perpendicular to that of the duct, the Coriolis force throws fast-moving core flow in the direction of the cross product of the mean velocity and the rotation vectors. The near-wall flow is driven from the pressure side to the suction side of the duct along the wall regions to satisfy the continuity conditions. This onset of a secondary flow leads to an increase in the average value of the friction factor and of the wall heat transfer rate. The earliest work on this subject focused on theoretical investigations of laminar flow in 'weakly rotating' circular pipes. By using a perturbation expansion, Baura (1954) and Benton (1956) showed that the secondary flow consisted of a counter-rotating double-vortex configuration. With a substantial increase in rotational speed at sufficiently high Reynolds numbers, Speziale (1982), and Kheshgi and Scriven

(1985) found that the usual counter-rotating double-vortex configuration breaks down into asymmetric four-vortex configuration. Yang *et al.* (1995) reviewed in detail the literature on rotating duct flow.

Since longitudinal curvature plays a role similar to that of spanwise rotation, analogous flow patterns can be observed in the fully developed laminar flow of a stationary curved duct. When a viscous fluid flows through a curved duct, the streamline curvature generates a centrifugal force that acts perpendicular to the main flow and produces a secondary flow. This double counter-rotating secondary flow causes the symmetric and quasi-parabolic axial velocity profile to become asymmetric, shifting the location of the maximum axial velocity outward. The first major theoretical study of laminar flow in a curved duct was performed by Dean (1927), who showed that the fully developed laminar flow in 'loosely curved' ducts depends largely on a single dimensionless parameter, now known as the Dean number. Humphrey *et al.* (1977) used LDA (laser-Doppler anemometry) to measure the velocity field, and confirmed that the location of maximum velocity moved from the centerline to the outer wall in a curved duct. Berger *et al.* (1983) extensively reviewed the secondary flow driven by centrifugal forces in a curved pipe.

To the best of the author's knowledge, most previous studies of the analogy between the two flows through orthogonally rotating straight ducts and stationary curved ducts have been performed on a qualitative basis. For example, Trefethen (1957) showed that variations of the friction factor due to the secondary flow patterns in both rotating and curved pipes could be expressed in terms of the Reynolds number and a dimensionless parameter characterizing each flow, but he did not provide a theoretical explanation. Ito and Nanbu (1971), and Ito (1959) derived dimensionless parameters for these flows by means of an integral method, but they did not mention any relationships between these parameters. In an earlier study of the authors of this work (2001), a quantitative analogy of the fully developed laminar flows in orthogonally rotating square ducts and stationary curved square ducts was confirmed through the physically reasonable dimensionless parameters. The objective of this study is to show that such a quantitative analogy can be established for rectangular ducts of arbitrary aspect ratio. Based on the similarity of the two flows, it would be possible to predict the flow characteristics in rotating ducts by considering flows in stationary curved ducts, and vice versa.

GOVERNING EQUATIONS

The Cartesian coordinate system fixed to a straight duct which rotates about *y*-axis at a constant angular velocity *W* and the cylindrical coordinate system where the radius of curvature along the duct centerline is represented by *R* are used for flow analysis in a rotating duct and a curved duct of rectangular cross-section as shown in Fig. 1(a) and 1(b) respectively. Due to space limitation, only the dimensionless governing equations for laminar, incompressible flows are considered briefly. More detailed derivation can be found in previous paper (Lee and Baek, 2001).

Rotating Straight Duct;

$$\frac{\partial \tilde{u}}{\partial \tilde{x}} + \frac{\partial \tilde{v}}{\partial \tilde{y}} = 0 \tag{1}$$

$$\frac{\partial \tilde{u}}{\partial \tilde{t}} + \tilde{u}\frac{\partial \tilde{u}}{\partial \tilde{x}} + \tilde{v}\frac{\partial \tilde{u}}{\partial \tilde{y}} = -\frac{\partial \tilde{p}^*}{\partial \tilde{x}} + \frac{1}{K_{LR}}\left(\frac{\partial^2 \tilde{u}}{\partial \tilde{x}^2} + \frac{\partial^2 \tilde{u}}{\partial \tilde{y}^2}\right) + 2\tilde{w} \tag{2}$$

$$\frac{\partial \tilde{v}}{\partial \tilde{t}} + \tilde{u}\frac{\partial \tilde{v}}{\partial \tilde{x}} + \tilde{v}\frac{\partial \tilde{v}}{\partial \tilde{y}} = -\frac{\partial \tilde{p}^*}{\partial \tilde{y}} + \frac{1}{K_{LR}}\left(\frac{\partial^2 \tilde{v}}{\partial \tilde{x}^2} + \frac{\partial^2 \tilde{v}}{\partial \tilde{y}^2}\right) \tag{3}$$

$$\frac{\partial \tilde{w}}{\partial \tilde{t}} + \tilde{u}\frac{\partial \tilde{w}}{\partial \tilde{x}} + \tilde{v}\frac{\partial \tilde{w}}{\partial \tilde{y}} = \tilde{C}_1 + \frac{1}{K_{LR}}\left(\frac{\partial^2 \tilde{w}}{\partial \tilde{x}^2} + \frac{\partial^2 \tilde{w}}{\partial \tilde{y}^2}\right) - \frac{2}{Ro}\tilde{u} \tag{4}$$

where p^* is the modified pressure given by

$$p^* = p - \frac{1}{2} r\Omega^2 (x^2 + z^2) \tag{5}$$

Since the pressure gradient in the main flow direction is invariant in the fully developed region, it follows that

$$-\frac{\partial p^*}{\partial z} = C_1 \tag{6}$$

where C_1 is a constant. In Eqs.(2)-(4), the Rossby number, $Ro=w_m/Wd$, is a convenient parameter for quantifying the relative strength of the inertial force to the Coriolis force acting on the fluid. Another dimensionless parameter $K_{LR}=Re/(Ro)^{1/2}$ represents the Reynolds number based on the velocity scale of the secondary flow $U_{SR}=w_m/(Ro)^{1/2}$. If a 'weakly rotating' duct flow is assumed for $Ro>8$, the limiting forms of Eqs.(2)-(4) do not include *Ro*, and the flow characteristics of the rotating duct are governed only by K_{LR}.

Stationary Curved Duct;

$$\frac{\partial \tilde{u}}{\partial \tilde{x}} + \frac{\partial \tilde{v}}{\partial \tilde{y}} = 0 \tag{7}$$

$$\frac{\partial \tilde{u}}{\partial \tilde{t}} + \tilde{u}\frac{\partial \tilde{u}}{\partial \tilde{x}} + \tilde{v}\frac{\partial \tilde{u}}{\partial \tilde{y}} - \tilde{w}^2 = -\frac{\partial \tilde{p}}{\partial \tilde{x}} + \frac{1}{K_{LC}}\left(\frac{\partial^2 \tilde{u}}{\partial \tilde{x}^2} + \frac{\partial^2 \tilde{u}}{\partial \tilde{y}^2}\right) \tag{8}$$

$$\frac{\partial \tilde{v}}{\partial \tilde{t}} + \tilde{u}\frac{\partial \tilde{v}}{\partial \tilde{x}} + \tilde{v}\frac{\partial \tilde{v}}{\partial \tilde{y}} = -\frac{\partial \tilde{p}}{\partial \tilde{y}} + \frac{1}{K_{LC}}\left(\frac{\partial^2 \tilde{v}}{\partial \tilde{x}^2} + \frac{\partial^2 \tilde{v}}{\partial \tilde{y}^2}\right) \tag{9}$$

$$\frac{\partial \tilde{w}}{\partial \tilde{t}} + \tilde{u}\frac{\partial \tilde{w}}{\partial \tilde{x}} + \tilde{v}\frac{\partial \tilde{w}}{\partial \tilde{y}} = \tilde{C}_2 + \frac{1}{K_{LC}}\left(\frac{\partial^2 \tilde{w}}{\partial \tilde{x}^2} + \frac{\partial^2 \tilde{w}}{\partial \tilde{y}^2}\right) \tag{10}$$

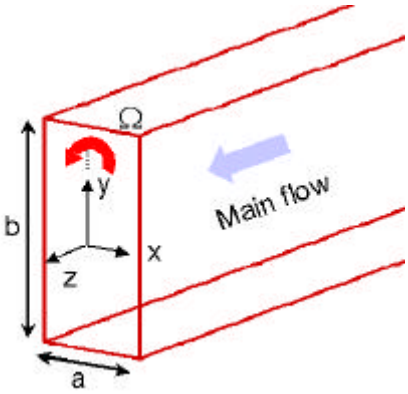

(a) Rotating straight duct

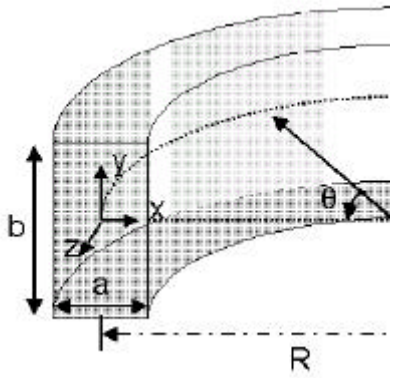

(b) Stationary curved duct

Fig. 1 Schematic and coordinate system for flow analysis

In the fully developed region, it follows that

$$-\frac{\partial p}{\partial z} = -\frac{1}{R}\frac{\partial p}{\partial q} = C_2 \qquad (11)$$

where C_2 is a constant. In Eqs. (7)-(10), $K_{LC}=Re/l^{1/2}$ represents the Dean number that corresponds to the Reynolds number based on the velocity scale of secondary flow $U_{SC}=w_m/l^{1/2}$ and the length scale d. Previous researches on finite curvature effects (Ito, 1959; Austin and Sieder, 1973) demonstrated that the effects of curvature ratio $l=R/d$ (which denotes the ratio of the inertial force to the centrifugal force) were practically negligible when l was larger than about 8. Therefore, Eqs.(7)-(10) are not a function of l, and the flow features exhibit an 'asymptotic invariance property' (which means K_{LC} is the sole governing parameter). It can be deduced from the above dimensionless governing equations that K_{LR} and Rossby number Ro for rotating duct flows correspond to Dean number K_{LC} and the curvature ratio l for the stationary curved duct flows. Also, the limiting forms of Eqs.(1)-(4) for a 'weakly rotating' duct flow are similar to those for a 'loosely curved' duct flow, except for body force terms, as shown in Eqs.(7)-(10).

NUMERICAL METHOD

The fractional step method used here is different from iterative projection methods (e.g. SIMPLE (Patankar and Spalding, 1972), PISO (Issa, 1986)) in that the projection of a tentative velocity onto the divergence free field is carried out at a time. In convection-diffusion step, the velocity field is solved by advancing the momentum equations in time. Then a Poisson equation, with the pressure as the dependent variable, is obtained by substituting the velocities into the continuity equation (continuity step); thus, the velocity field obtained at the previous time step is projected onto a divergence-free space. This equation is formulated such that the continuity equation will be satisfied at the next time level. In steady flow calculation, the solution is advanced in pseudo-time until a convergence is reached. This allows the Poisson equation to be simplified for the continuity step, and avoids odd-even decoupling associated with the use of a non-staggered grid, while minimizing errors in the discrete pressure-Poisson equation. Second-order accurate central differencing is used to discretize the viscous and pressure gradient terms, and second-order accurate upwind differencing is used to minimize the cross-stream numerical diffusion for the convective term. The use of upwind differencing scheme for the convection term also eliminates the need for adding artificial dissipation terms in the momentum equations to stabilize the numerical algorithm. All the equations are solved using the ADI method. A local time stepping is used to accelerate the convergence of the solution. The use of a non-staggered grid simplifies the implementation of boundary conditions and reduces the storage requirements of the variables. Due to the symmetric configuration of the flow, the computation is performed in only a half-domain of the cross-section with the symmetric boundary condition. At the wall, no slip boundary condition is applied. All velocity components are set to zero. The computations are performed on 35×18 nodes for square ducts, 35×35 nodes for A=2 rectangular ducts and 35×69 nodes for A=4 rectangular ducts. A non-uniform grid with clustering at the near wall region is employed due to the presence of a boundary layer near the wall, in which velocity changes rapidly for both the main and secondary flows. The accuracy of grid density and spacing was confirmed by previous study (Lee and Baek, 2001). The convergence criteria are set at a residual drop of 5 to 6 orders of magnitude in the solution variables between the present and previous time steps.

RESULTS

General flow patterns

Figure 2 shows the secondary velocity vectors and streamlines for aspect ratios A=2 and 4. The upper half of each duct cross-section corresponds to the curved duct flow, while the lower half shows the rotating duct flow. Pressure and suction side in rotating duct flows correspond to the outer (convex) and inner (concave) wall respectively. To illustrate

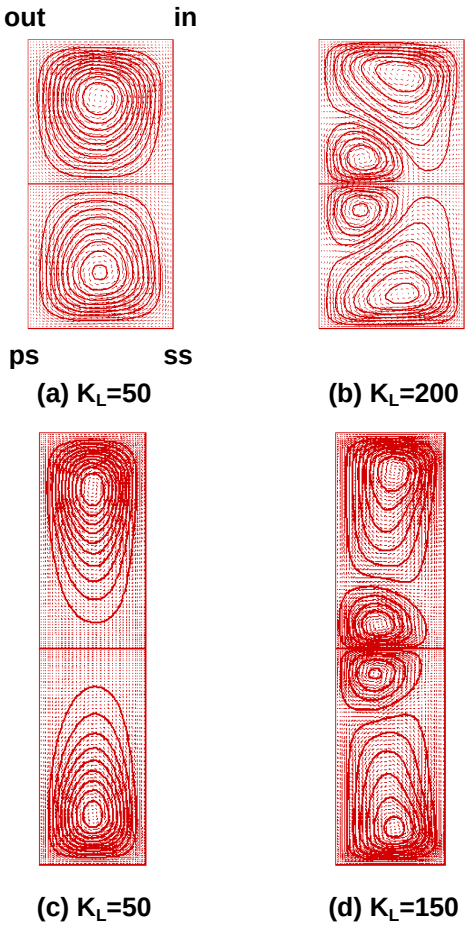

Fig. 2 Secondary velocity vectors and streamlines for Ro=10 and l=10 ((a),(b); A=2, (c),(d); A=4)

the onset of instability, the flow patterns before and after the flow instability are shown in Fig. 2. For a rotating duct, when K_{LR} is small (Fig. 2(a), (c)), the secondary flow consists of a counter-rotating double-vortex configuration. As the magnitude of K_{LR} increases (Fig. 2(b), (d)), the existing double-vortex breaks down into an asymmetric structure of four counter-rotating vortices. The subsidiary counter-rotating vortex pair that is called Coriolis vortices (Hart, 1971; Yang *et al.*, 1994) on the pressure side results from a disparity in the balance of the pressure gradient and the Coriolis force. In a stationary curved duct, the centrifugal force is proportional to the square of the axial velocity at a given position. The inviscid flow in the central core region, which has the highest momentum, is subjected to a larger centrifugal force than the slower-moving fluid in the neighborhood of the duct walls. In order to achieve a momentum balance in the radial direction, the magnitude of the radial velocity component (u) changes accordingly within the inviscid core region. Therefore, in the middle of the duct, the fluid moves away from the center of curvature, whereas the fluid near the upper and lower walls moves towards the center of curvature. These velocity distributions result in a counter-rotating double vortex (which are called Ekman vortices) configuration (Fig. 2(a), (c)). Similar to a rotating straight duct, due to an imbalance between the pressure gradient and the centrifugal force, an additional vortex pair which are called Dean vortices (Dean, 1927) appear near outer wall above the critical values of K_{LC} (Fig. 2(b), (d)).

Figure 3 shows the non-dimensionalized axial velocity (w/w_m) contours. For rotating duct flows, as the magnitude of K_{LR} increases, the high-momentum fluid, originally in the central core, is convected to the pressure side of the duct, leading to a significant reduction in the thickness of the boundary layers along the pressure and bottom sides, while the low-momentum fluid accumulates along the suction side, causing the boundary layer thickness to increase. In curved duct flows, the location of the maximum axial velocity shifts toward the outer wall by the centrifugal force that acts outwards from the center of curvature. For each value of K_L, the patterns of the two flows are similar.

The axial velocity profiles along the horizontal centerlines of both ducts for Ro and l equal to 10 are shown in Fig. 4. In

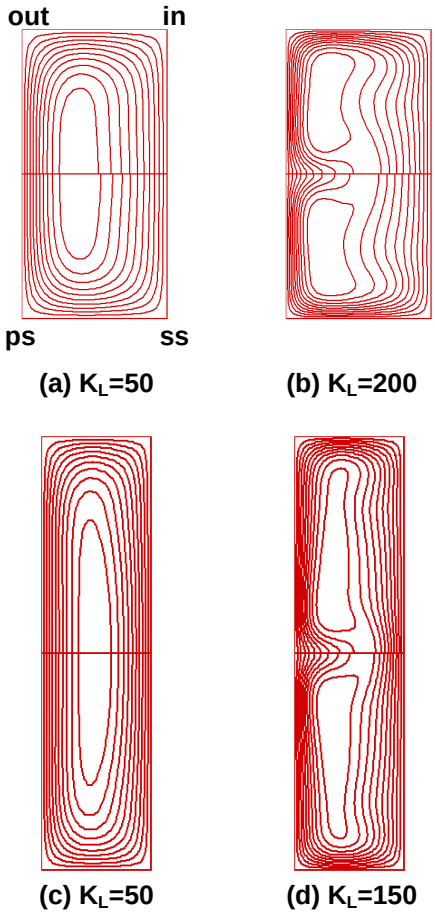

Fig. 3 Non-dimensionalzed axial velocity contours for Ro=10 and l=10 ((a),(b); A=2, (c),(d); A=4)

Fig. 4(a), when A=2 and K_L=10, the secondary flow is too weak to affect the main flow. The velocity profile is essentially symmetric and parabolic, with the maximum value occurring at or very close to the center of the duct. As K_L increases to 50 and 125, the velocity profiles gradually become asymmetric and the maximum axial velocity shifts toward the pressure side. With a further increase in K_L from 125 to 175, the peak velocity drops considerably and shifts towards the suction side. When K_L increases to 300, the peak once again moves slightly toward the center of the duct. For A=4, the peak velocity drops and shifts towards the suction side in lower critical value of K_L compared to A=2 (Fig. 4(b)). This result implies that, in the case of higher aspect ratio, the onset of flow instability occurs at a much lower value of K_L.

Friction factors

One of the most important practical aspects of duct flow is an estimation of the friction factor. The friction factors f of these two flows, normalized by the corresponding value for a stationary straight duct f_0, increase with K_L as shown in Fig. 5. This monotonic increase in the friction factor ratio with K_L shows that the enhanced effects of rotation and curvature increase the intensity of secondary flow. Good agreement with previous results (Cheng and Akiyama, 1970; Cheng *et al.*, 1976; Ghia and Sokhey, 1977; Thangam and Hur, 1990) is evident from the figure.

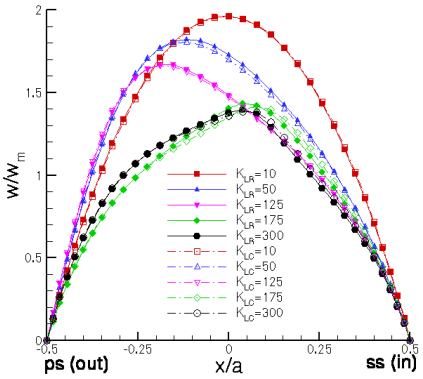

(a) A=2

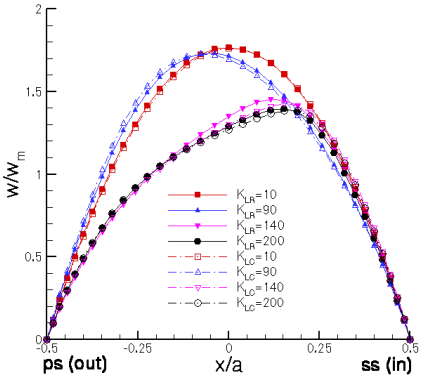

(b) A=4

Fig. 4 Axial velocity profiles along the horizontal centerline of the duct (Ro=10 and l=10)

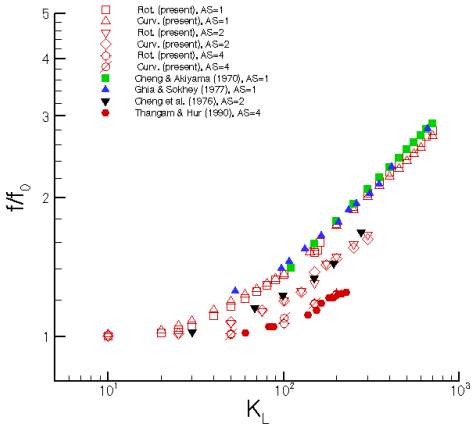

Fig. 5 Friction factor ratio

Other flow features

In order to examine how well the 'asymptotic invariance property' of the dimensionless parameter K_L is satisfied for each flow when Ro or l are very large, two additional computations were performed for A=1 at Ro and l equal to 50 and 100. Figure 6 shows the variation of the maximum axial velocity (w_{max}/w_m) with K_L. The magnitudes of w_{max}/w_m at Ro and l equal to 50 and 100 are the same as those found when Ro and l=10. Therefore, the maximum axial velocity is independent of the magnitude of Ro and l, and an 'asymptotic invariance property' of K_L exists when Ro or l is larger than about 8. The magnitudes of the peak velocity in each flow are nearly the same, except at the critical value of K_L where a discontinuity exists.

The variation of the normalized maximum value of the secondary flow velocity V_{Smax} (which is called the secondary flow intensity) with K_L is shown in Fig. 7. The difference between the V_{Smax} of the two flows is greater than observed for an integral property such as the friction factor (Fig. 5). This discrepancy arises because the Coriolis force on a fluid is proportional to its velocity, whereas the centrifugal force on a fluid is proportional to its velocity square. The secondary flow intensity experiences a sudden decrease near the onset of the transition from the double- to four-vortex flow pattern. As the aspect ratio increases, the difference of secondary flow intensity between the two flows is reduced. The magnitude of secondary flow intensity is also reduced with a higher aspect ratio. This result explains the reason why the friction factors f decrease with aspect ratios as shown in Fig. 5.

CONCLUSIONS

Detailed numerical studies were performed in order to investigate the quantitative analogy of the fully developed laminar flows in orthogonally rotating rectangular ducts and

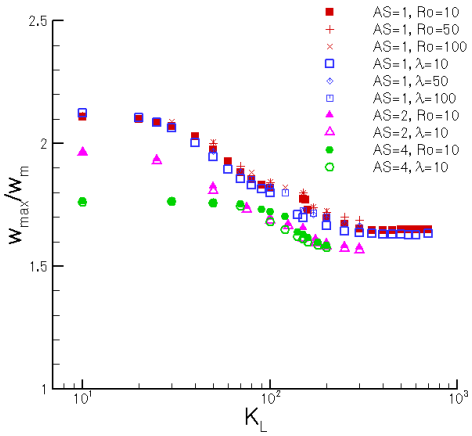

Fig. 6 Variation of the maximum axial velocity ratio with K_L

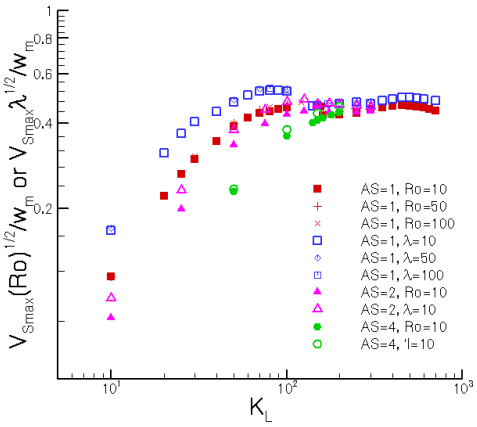

Fig. 7 Variation of the secondary velocity intensity with K_L

stationary curved rectangular ducts of arbitrary aspect ratios by employing a high-order accurate numerical scheme. The following conclusions were made:

1) K_{LR} and the Rossby number *Ro* for rotating duct flows corresponded to the Dean number K_{LC} and curvature ratio l for stationary curved duct flows.
2) When the magnitude of *Ro* and l were greater than about 8, K_{LR} and K_{LC} became the sole governing parameters in each flow, clearly establishing the quantitative similarities between the two flows.
3) The friction factor and primary flow patterns of the two flows coincide for a wide range of K_L. Flow variables, normalized using proper scales such as the maximum axial velocity or secondary velocity intensity of two flows, exhibit similar behavior. Therefore, based on the results of the present study, it is expected that the flow characteristics in orthogonally rotating rectangular duct of arbitrary aspect ratio can be predicted by considering flows in stationary curved rectangular ducts, and vice versa.

ACKNOWLEDGMENTS

This work was partially supported by the Brain Korea 21 Project and the authors gratefully thank Dr. Ishigaki for some valuable comments during the 'Winter Institute Program' supported by the Japan-Korea Industrial Technology Cooperation Foundation.

REFERENCES

Austin, L. R., and Seader, J. D., 1973, "Fully developed Viscous Flow in Coiled Circular Pipes," AIChE J., **19**, pp. 85-93

Baura, S. N.,1954, "Secondary Flow in a Rotating Straight Pipe," Proc. R. Soc. Lond. , **A 227**, pp. 133-139

Benton, G. S., 1956, "The Effect of the Earth's Rotation on Laminar Flow in Pipes," J. Appl. Mech., **23**, pp. 123-127

Berger, S. A., Tabolt, L., and Yao, L.-S., 1983, "Flow in Curved Pipes," Ann. Rev. Fluid Mech., **15**, pp. 461-551

Cheng, K. C., and Akiyama, M., 1970, "Laminar Forced Convection Heat Transfer in Curved Rectangular Channels," Int. J. Heat Mass Transfer, **13**, pp. 471-490

Cheng, K. C., Lin, R.C., and Ou, J. W., 1976, "Fully Developed Laminar Flow in Curved Rectangular Channels," J. Fluids Eng., **98**, pp. 41-48

Dean, W. R., 1927, "Note on the Motion of Fluid in a Curved Pipe," Phil. Mag., **4**, pp. 208-223

Ghia, K. N., and Sokhey, J. S., 1977, "Laminar Incompressible Viscous Flow in Curved Ducts of Regular Cross-Sections," J. Fluids Eng., **99**, pp. 640-648

Hart, J. E., 1971, "Instability and Secondary Motion in a Rotating Channel Flow," J. Fluid Mech., **45**, pp. 341-353

Humphrey, J. A. C., Taylor, A. M. K., and Whitelaw, J. H., 1977, "Laminar Flow in a Square Duct of Strong Curvature," *J. Fluid Mech.*, **83**, pp. 509-527

Issa, R. I., 1986, "Solution of the Implicitly Discretized Fluid Flow Equation by Operator-Splitting," J. Comp. Phys., **59**, pp. 308-23.

Ito, H., 1959, "Friction Factors for Turbulent Flow in Curved Pipes," J. Basic Eng., **81**, pp. 123-134

Ito, H., and Nanbu, K., 1971, "Flow in Rotating Straight Pipes of Circular Cross Section," J. Basic Eng., **93**, pp. 383-394

Kheshgi, H. S., and Scriven, L. E., 1985, "Viscous Flow through a Rotating Square Channel," Phys. Fluids, **28**, pp. 2868-2979

Lee, G. H., and Baek, J. H., 2001, "Similarity Comparison of Laminar Flows in Orthogonally Rotating Square Duct and Stationary Curved Square Duct," Int. J. Rotating Machinery, (in press)

Patankar, S. V., and Spading, D. B., 1972, "A Calculation Procedure for Heat, Mass and Momentum Transfer in Three-Dimensional Parabolic Flows," Int. J. Heat & Mass Transfer, **15**, pp. 1787-1806.

Speziale, C. G., 1982, "Numerical Study of Viscous Flow in Rotating Rectangular Ducts," J. Fluid Mech., **122**, pp. 251-271

Thangam, S., and Hur, N., 1990, "Laminar Secondary Flows in Curved Rectangular Ducts," J. Fluid Mech., **217**, pp. 421-440

Trefethen, L. M., 1957, Flow in Rotating Radial Ducts, General Electric Report, No. 55GL350-A

Yang, W. J., Fann, S., and Kim, J. H., 1994, "Heat and Fluid Flow inside Rotating Channels," Appl. Mech. Rev., **47**, pp. 367-396